Computational modeling of breakdown process in RF plasmas

IEPC-2025-410

Presented at the 39th International Electric Propulsion Conference Imperial College London, London, UK September 14-19, 2025

Yusuke Yamashita¹, Vedanth Sharma², and Kentaro Hara³ Stanford University, Stanford, California 94305

Single- and dual-frequency ratio frequency (RF) breakdown are investigated using two one-dimensional (1D) kinetic models: the electron Monte Carlo (E-MC) model and the particle-in-cell Monte Carlo collision (PIC-MCC) model. The E-MC model considers only electrons, and the electric field is assumed to be a Laplace solution (i.e., no space charge), while the PIC-MCC model considers both electrons and ions and the Poisson equation is self-consistently solved. Both the E-MC model and the PIC-MCC simulation model consider the electron-induced secondary electron emission (EI-SEE) and ion-induced electron emission (IIEE). For single-frequency RF breakdown at 27.12 MHz, the breakdown voltages obtained from the E-MC model agree with experimental data when accounting for SEE, inelastic reflection, and elastic reflection. For dual-frequency breakdown at 27.12 MHz and 2 MHz, the breakdown voltages of 27.12 MHz obtained from the E-MC model and PIC-MCC model are in good agreement with the experimental data at various constant voltages of 2 MHz when accounting for the appropriate IIEE coefficient. The PIC-MCC simulation results show that the incident ion flux at the electrodes depends on the RF cycle of 2 MHz, indicating that the effective ion-induced electron emission is different from the E-MC simulation.

I. Introduction

Plasma initiation, i.e., breakdown, occurs when applying a voltage larger than the minimum voltage to sustain the plasma [1]. Gas breakdown is an important phenomenon in electric propulsion (EP) devices for cathode initiation, initial transient, and anomalous arcing. The difference between the plasma initiation and steady-state operation could become a restriction on designing the power supply for space missions. In addition, undesired breakdown has been observed in EP devices (e.g., between the screen grid and accelerator grid in gridded ion thrusters [2]), which is one potential cause of the thruster system failure. Hence, better understanding of the breakdown process is important for EP community.

Gas breakdown is a phenomenon when gas starts conducting by generating a self-sustaining plasma. In direct-current (DC) discharges, the breakdown voltage is function of pd, where p and d are pressure and distance of anode-cathode gap (cf. Paschen theory) [3]. Gas breakdown have been studied by several discharges, including microgap discharges and ratio-frequency (RF) discharges. In the microgap discharges, the breakdown characteristics is different from the Paschen theory at low pd due to the presence of field emission [1, 4–6]. In single-frequency RF discharges, several experimental and numerical works suggest that the breakdown condition is also a function of fd and show the multi-valued breakdown characteristics at low pd regime, where f is the frequency of RF voltage [7–12]. In dual-frequency RF discharges, an experimental work and a numerical work show that the high frequency (HF) breakdown voltages are obtained when applying several constant low frequency (LF) voltages at 27.12 MHz and 2 MHz [8, 13]. Furthermore, non-uniform geometry (e.g., pin to plate) [6, 14], electrical circuit [15, 16], and gas mixture [17, 18] also affect the breakdown characteristics. To predict the breakdown characteristics involving many physical and chemical processes, high-fidelity plasma modeling is required.

For computational modeling of RF breakdown, two kinetic models, namely, PIC-MCC simulation and electron Monte Carlo (E-MC) simulation, are often utilized [9–11, 13, 15, 16, 19–22]. The PIC-MCC model takes into account

¹Postdoctoral Researcher, Aeronautics and Astronautics, yamashita.yusuke@jaxa.jp.

²Ph.D. Candidate, Aeronautics and Astronautics, vedanth@stanford.edu

³Assistant Professor, Aeronautics and Astronautics, kenhara@stanford.edu

for both ion and electron trajectories, solving the Poisson equation with the space charge effects. On the other hand, an E-MC simulation considers only electron trajectories with the Laplace equation without the space charge effects. The breakdown conditions are typically obtained in the limit of initial small space charge [1] (cf. Townsend discharge), the assumption without space charge effects might be valid. In general, the computational cost of E-MC simulation is much cheaper than the PIC-MCC simulation that considers the ion trajectories because of the difference in time scale between electrons and ions. For the single-frequency breakdown, E-MC simulations can capture the experimental observations of breakdown characteristics well [9–11, 13, 19]. Notably, an ion-induced electron emission (IIEE) model is proposed based on the number of ionization events, and show in a good agreement with the experimental data, although the ion dynamics is not simplified in the E-MC simulation [10, 11]. Furthermore, Ref. [13] considers the energy and angle dependent electron-induced secondary electron emission (SEE), including elastically backscattering, rediffusion (inelastic scattering), and true secondary [23] in the E-MC simulation, which shows good agreement with the experimental data. For the dual-frequency RF breakdown, the E-MC simulation that considers electron elastically backscattering and IIEE provides good agreement with experimental trends. In the E-MC simulation, the IIEE is based on Ref. [10], and the timing of IIEE is assumed to be random in time from powered and grounded electrodes. However, in reality, the ions are generated via the ionization and then takes time to reach the electrodes, resulting in IIEE. If the ion incident flux depends on the RF electric field (e.g., phase, frequency, voltage), the assumption of the E-MC simulation might be violated.

In this paper, PIC-MCC simulation and E-MC simulation are benchmarked and validated with the experimental data in the dual-frequency RF breakdown [8]. We perform the phase analysis of the ion incident flux to electrodes with respect to the voltage waveform in order to discuss the effective IIEE.

II. Numerical model

Two kinetic models are developed for single- and dual-frequency RF breakdown. Molecular nitrogen is considered as the background neutral gas with a temperature of 300 K based on experimental work [8]. The cross sections for electron-neutral collisions of molecular nitrogen are from the results of Phelps and Pitchford [24]. In this paper, 1D geometry is assumed, and we set the powered electrode at x = 0, and the grounded electrode at x = d. At the powered electrode, the dual-frequency RF voltage is employed, i.e., $V(x = 0, t) = V_{\text{HF}} \sin(2\pi f_{\text{HF}}t) + V_{\text{LF}} \sin(2\pi f_{\text{LF}}t)$. At the grounded electrode, V(x = d, t) = 0 is employed. The high frequency (HF), low frequency (LF), and the gap between the powered and grounded are assumed to be 27.12 MHz, 2MHz, and 2.04 cm, respectively, based on an experimental paper [8]. For both E-MC model and PIC-MCC model, the electron-neutral collision is considered via the Monte Carlo collision (MCC) with null collision algorithm [25].

A. E-MC model

The E-MC simulation considers only electron trajectories with the Laplace equation, assuming that the space charge effects are negligible, which is typically a valid assumption for breakdown (cf. Townsend discharge) [1].

$$E(t) = \frac{V_{\text{HF}}}{d}\sin(2\pi f_{\text{HF}}t) + \frac{V_{\text{LF}}}{d}\sin(2\pi f_{\text{LF}}t),\tag{1}$$

where E is the electric field that is uniform between the electrodes. The simulation time step for the particle update is $\Delta t = 1/(8000 f_{\rm HF}) \approx 4.6$ ps. The number of initial electrons is set to be 2×10^5 and 10^6 for the single- and dual-frequency RF breakdown based on a particle convergence study, respectively. Initially, electron macroparticles are located at the ground electrode (x/d = 1). It should be noted that the initial position of electron macroparticles [9] does not affect the breakdown voltage.

B. PIC-MCC model

Both ions and electrons trajectories are self-consistently considered. In this paper, only N_2^+ is considered for ions. The isotropic scattering is assumed for the electron-neutral collisions. V(x,t) is self-consistently obtained by solving the Poisson equation using a tridiagonal matrix solver.

At the initial condition, the uniform plasma density of n_{p0} is assumed. The electron and ion velocities are obtained from the Maxwellian distribution with the electron temperature of 3 eV and the ion temperature of 300 K, respectively. The breakdown condition corresponds to the Townsend regime, and the plasma density is pretty low. Hence, in the present work, $n_{p0} = 10^8 \text{ m}^{-3}$ is used so that the breakdown condition does not depend on the initial plasma

density [1], which is similar condition of previous RF breakdown simulations using PIC-MCC [16, 20]. The initial number of for both electron and ion macroparticles are set to be 2×10^5 from the particle convergence study. The grid size is set to be $\Delta x = d/64$. It should be noted that the grid size well satisfies $\Delta x/\lambda_D < 1$ for all cases from the initial transient to the steady state. In this paper, we use a different time step for electron and ion, i.e., the sub-cycle method, to reduce the simulation cost. For electrons, the simulation time step is the same as the E-MC model (i.e., $\Delta t_e = 1/(8000 f_{\rm HF}) \approx 4.6$ ps). On the other hand, the time step of ions $\Delta t_i = 1/(20 f_{\rm HF}) = 400 \Delta t_e$. The breakdown condition corresponds to the Townsend regime, where n_i is two or three orders of magnitude larger than n_e because of small space charge effects [1]. Hence, the subcycle method can reduce the simulation cost significantly if the same macroparticle weight is used for ions and electrons.

C. Electron emission from electrodes

1. Electron-induced SEE

An energy and angle dependent electron-induced SEE model is considered, which includes the elastically backscattering, rediffusion, and true secondary [23].

$$\delta_t(\varepsilon_e, \theta) = \rho_e(\varepsilon_e, \theta) + \rho_r(\varepsilon_e, \theta) + \gamma_e(\varepsilon_e, \theta), \tag{2}$$

where ρ_e is the elastic backscattering coefficient, ρ_r is the rediffusion coefficient, and γ_e is the true secondary electron emission coefficient. In this paper, the stainless steel condition is assumed for the electrodes. First, the elastic reflection, rediffusion, or true secondary are determined based on a random number [13], and then the post-collisional velocity is determined. For elastic backscattering, Additionally, based on the type of electron reflection and emission, the post-collisional velocity needs to be determined. For rediffusion, the post-collisional electron energy is chosen as $\varepsilon_{e,post} = R\varepsilon_{e,pre}$, where R is a random number uniformly distributed between 0 and 1, where $\varepsilon_{e,pre}$ and $\varepsilon_{e,post}$ are the energy of incident and reflected electrons, respectively. Then, the electrons are emitted assuming the half-Maxwellian distribution. Here, the effective electron temperature for the half-Maxwellian is set to be $T_{e,post} = \varepsilon_{e,post}/2$ so that the average electron energy for the emitted electrons is close to $\varepsilon_{e,post}$. Finally, the velocity of true secondary emission is chosen from a half-Maxwellian with a temperature of 2.5 eV.

2. Ion-induced electron emission (IIEE)

In this paper, we use several constant coefficients for IIEE, γ_i . For the PIC-MCC simulation, an electron is emitted with the probability of γ_i when an ion collides with the electrodes. In contrast, the E-MC simulation considers the IIEE via the number of ionization events. Considering that ions eventually reach the electrodes for electropositive plasmas, the electron flux from the electrodes due to IIEE can be written, from particle balance, as [11],

$$\int_{kT_{\rm HF}}^{(k+1)T_{\rm HF}} \Gamma_{e,\rm IIEE} dt = \gamma_i N_{\rm iz}, \tag{3}$$

where $T_{\rm HF} = f_{\rm HF}^{-1}$ is the HF cycle, N_{iz} is the number of ionization integrated over one HF cycle between $t = (k-1)T_{\rm HF}$ and $t = kT_{\rm HF}$, and γ_i is the IIEE coefficient. In the present work, we integrate the number of ionizations over one HF cycle, and then electrons are injected at the next HF cycle. The emitted electrons are assumed to be introduced randomly in time and from the powered and grounded electrodes. The electron velocity distribution function (EVDF) is assumed to be half-Maxwellian with the electron temperature of 2.5 eV for both PIC-MCC simulation and E-MC simulation.

D. Automatic method to breakdown voltage

The HF breakdown voltage is determined based on the growth or damp of space-averaged ion density and electron density. The breakdown condition can be achieved when $\partial \langle n_i \rangle / \partial t \approx 0$ and $\partial \langle n_e \rangle / \partial t \approx 0$ at the steady-state. The simulation time is needed to be set large enough to see growth or damp of ion and electron densities. For the E-MC simulation, $t = 160T_{\rm HF}$ for single-frequency RF breakdown and $t \approx 271T_{\rm HF}$ (i.e., $t = 20T_{\rm LF}$ are used, where $T_{\rm LF} = f_{\rm LF}^{-1}$ is the LF cycle.) for dual-frequency RF breakdown, respectively. For the PIC-MCC simulation, $t = 110T_{\rm LF}$ is used for dual-frequency RF breakdown. This indicates that the simulation time of PIC-MCC is approximately 5.5 times larger than the E-MC simulation since a longer time is required to reach steady-state for ions. The HF breakdown voltage is determined by an automatic method similar to the Newton's root-finding method [1, 13, 26]. After several iterations, $\langle \partial n_e / \partial t \rangle \approx 0$ and $\langle \partial n_i / \partial t \rangle \approx 0$ can be achieved at the steady-state.

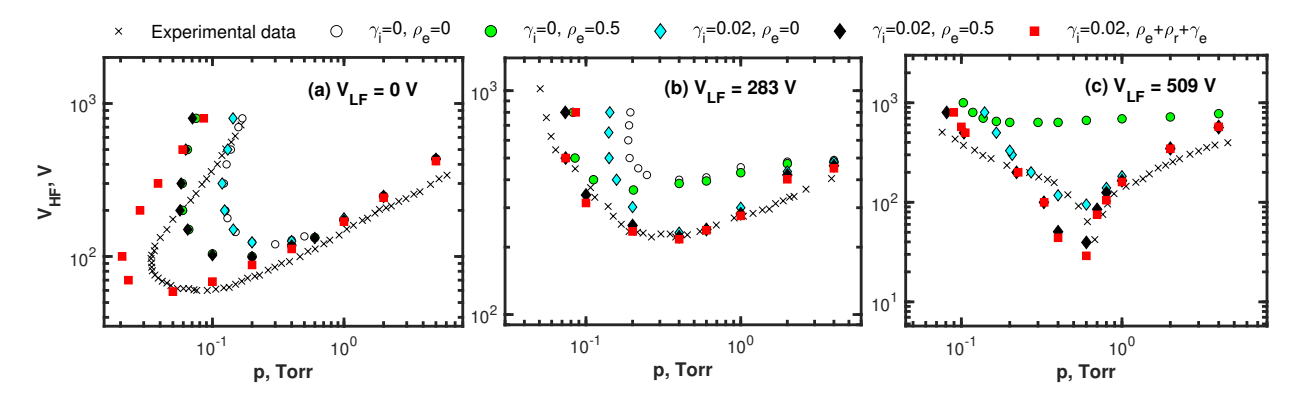


Fig. 1 HF breakdown voltages obtained from E-MC simulation when applying (a) $V_{LF} = 0$ V, (b) $V_{LF} = 283$ V and (c). $V_{LF} = 509$ V. Five cases are shown using different combinations of ion-induced electron emission (IIEE) and the electron-induced secondary electron emission (EI-SEE): (i) $(\gamma_i, \rho_e) = (0, 0)$; (ii) $(\gamma_i, \rho_e) = (0, 0.5)$; (iii) $(\gamma_i, \rho_e) = (0.02, 0)$; (iv) $(\gamma_i, \rho_e) = (0.02, 0.5)$; and (v) $\gamma_i = 0.02$ with the energy- and angle-dependent EI-SEE model assuming isotropic scattering $(\rho_e + \rho_r + \gamma_e)$. Experimental data are extracted from Ref. 8. Simulation results are reproduced from Ref. 13.

III. Electron-Monte Carlo simulation results

Figure 1 shows (a) single-frequency RF breakdown at $V_{\rm LF}=0$ V, (b) dual-frequency RF breakdown at $V_{\rm LF}=283$ V, and (c) dual-frequency RF breakdown at $V_{\rm LF}=509$ V. Five cases of the breakdown voltage obtained from the E-MC simulation, which is compared with the experiment in Ref. [13]. The five simulation cases are (i) no electron emission ($\gamma_i=0$ & $\rho_e=0$), (ii) elastic backscattering only ($\gamma_i=0$ & $\rho_e=0.5$), (iii) IIEE only ($\gamma_i=0.02$ & $\rho_e=0$), (iv) constant IIEE and elastic backscattering ($\gamma_i=0.02$ & $\rho_e=0.5$), and (v) constant $\gamma_i=0.02$ with energy- and angle-dependent EI-SEE model ($\rho_e+\rho_r+\gamma_e$).

A. Single-frequency RF breakdown ($V_{LF} = 0 \text{ V}$)

Figure 1(a) indicates the breakdown voltages for all five cases show good agreement with the experimental data in the right branch (high pd, e.g., $p \ge 0.4$ Torr). However, the breakdown voltages deviate around the minimum voltage (e.g., $V_{\rm HF} < 100$ V) and in the left branch (low pd, e.g., $p \le 0.2$ Torr), suggesting that the electron emission from the electrodes plays an important role in the breakdown condition. The elastic reflection is important in the left branch from the small voltage to the high voltage. In addition, the rediffusion and true secondary are also important around the minimum voltage (e.g., $V_{\rm HF} < 100$ V). Ref. [13] discusses how the EI-SEE affects the breakdown condition based on the phase analysis of the electron incident flux relative to the voltage waveform. At low pd and around the minimum voltage (e.g., $V_{\rm HF} < 100$ V), the emitted electrons due to rediffusion and true secondary can be utilized effectively for the ionization.

B. Dual-frequency RF breakdown ($V_{LF} = 283 \text{ V}$ and $V_{LF} = 509 \text{ V}$)

For $V_{\rm LF}=283$ V, as shown in Fig. 1(b), in the higher pd regime ($p \ge 0.4$ Torr), the breakdown characteristics are influenced by IIEE but not EI-SEE. in the lower pd regime ($p \le 0.2$ Torr), the elastic reflection is important, while the rediffusion and true secondary emission do not affect dual-frequency RF breakdown. Ref. [13] shows that most of the emitted electrons due to EI-SEE cannot go to the bulk region because of the electric potential, while the IIEE can go to the bulk region and contribute to the ionization.

For $V_{\rm LF} = 509$ V, Fig. 1(c) indicates that the HF breakdown voltages are not found at $V_{\rm HF} \leq 1500$ V with Case (i), when no electron emission condition (γ_i =0 & ρ_e = 0), indicating that the electron emissions are necessary for dual-frequency with large $V_{\rm LF}$. When considering γ_i = 0.02, i.e., Cases (iii)-(v), the breakdown voltages obtained from the E-MC simulation start to capture the experimental trend. Interestingly, ρ_e is important in low pd regime similar to the single-frequency RF breakdown shown in Fig. 1(a). Finally, the rediffusion and true secondary are not important for the dual-frequency RF breakdown, which is similar to (b) $V_{\rm LF}$ = 283 V.

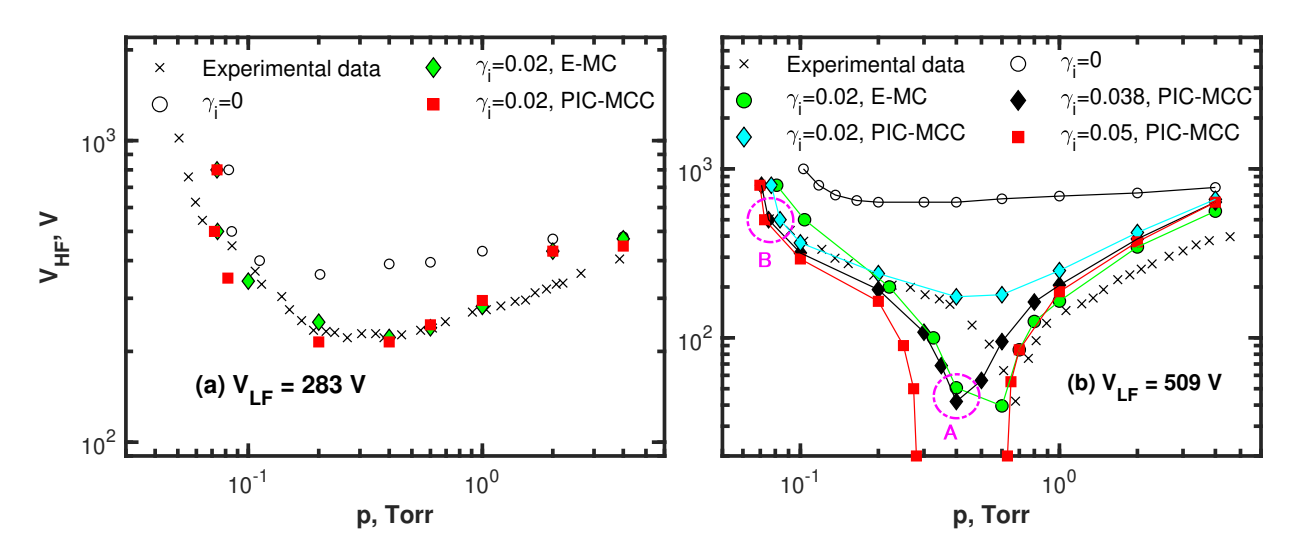


Fig. 2 Benchmark between E-MC simulation and PIC-MCC simulation for dual-frequency RF breakdown. The HF breakdown voltages when applying (a) $V_{\rm LF} = 283$ V and (b) $V_{\rm LF} = 509$ V. For all simulation conditions, $\rho_e = 0.5$ is considered. Details of the results at Points A and B are discussed in Fig. 3. Experimental data are extracted from Ref. 8. E-MC simulation results are reproduced from Ref. 13.

IV. PIC-MCC simulation results

The HF breakdown voltages at 27.12 MHz are obtained from the PIC-MCC simulation when applying $V_{\rm LF} = 283$ V and 509 V. The simulation results are benchmarked with the E-MC simulation [13] and validated with the experimental data [8]. For all simulation results, $\rho_e = 0.5$ is considered, while the rediffusion and true secondary are not considered for the comparison based on Fig. 1. Several γ_i are tested in the PIC-MCC simulation.

A. $V_{\rm LF} = 283 \ { m V}$

Figure 2(a) shows the HF breakdown voltages when $V_{\rm LF} = 283$ V. Three simulation conditions are shown (i) no IIEE ($\gamma_i = 0$), (ii) $\gamma_i = 0.02$ using E-MC, (iii). $\gamma_i = 0.02$ using PIC-MCC. For Case (i) no IIEE, the difference of PIC-MCC simulation and E-MC simulation is the space charge effects. However, the breakdown voltages are obtained in the limit of low density in the PIC-MCC simulation [1], the HF breakdown voltages obtained from PIC-MCC are identical to the E-MC simulation. In fact, the time-averaged potential is the order of initial ion temperature (e.g., 10^{-2} eV), which is negligibly smaller than the RF voltage. More importantly, Cases (ii) and (iii) show that the breakdown voltages obtained the PIC-MCC simulation are in good agreement with the E-MC simulation. This indicates that the contribution of RF discharge due to IIEE (cf. ionization) is comparable on average between the PIC-MCC and E-MC simulations.

B. $V_{\rm LF} = 509 \ { m V}$

Figure 2(b) shows the HF breakdown voltages when $V_{\rm LF} = 509$ V. Five simulation conditions are shown (i) no IIEE $(\gamma_i = 0)$, (ii) $\gamma_i = 0.02$ using E-MC, (iii). $\gamma_i = 0.02$ using PIC-MCC, (iv). $\gamma_i = 0.038$ using PIC-MCC, (v). $\gamma_i = 0.05$ using PIC-MCC. Most important observation from Cases (ii) and (iii) is that the HF breakdown voltages obtained from PIC-MCC simulation are in good agreement with the E-MC simulation at lower pd (e.g., $p \le 0.2$ Torr), while the deviation is observed around the minimum voltages (e.g., $0.2 Torr), which is different from <math>V_{\rm LF} = 283$ V as shown in Fig. 2(a). In order to get better agreement with the experiment near the minimum voltages using the PIC-MCC simulation, higher $\gamma_i = 0.038$ or $\gamma_i = 0.05$ (Cases (iv) and (v)) needs to be used. This indicates that the effective IIEE coefficient is not equal to the actual IIEE coefficient and depends on the LF voltage and pressure. The mechanism will be discussed later.

V. Phase of ion-induced electron emission

Figure 3 shows the voltage of the powered electrode (at x = 0), while the ground electrode is V = 0 at x = d, and the normalized incident ion flux that collides with the powered electrode $\Gamma'_{i,p}$ obtained from the PIC-MCC simulation,

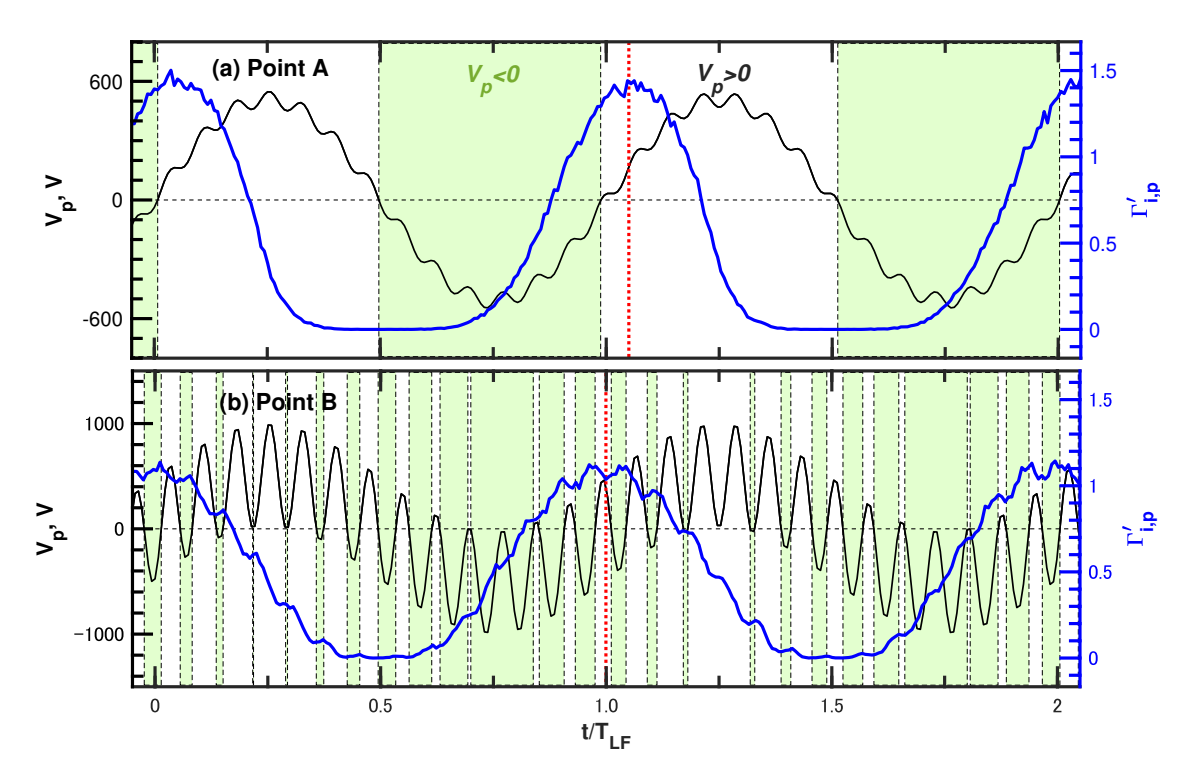


Fig. 3 Phase analysis of dual-frequency RF breakdown obtained from the PIC-MCC simulation. Normalized incident ion flux at powered electrode $\Gamma'_{i,p}$ (blue) with respect to the voltage waveform (black) when applying $V_{\rm LF} = 509$ V: (a) $V_{\rm HF} = 42$ V at p = 0.4 Torr with $\gamma_i = 0.038$ and (b) $V_{\rm HF} = 500$ V at p = 0.082 Torr with $\gamma_i = 0.02$. Green shadow regions correspond to $V_p(t) < 0$, where emitted electrons can be accelerated into the bulk region. Red line shows the time t^* when the integration of incident ion flux becomes half, i.e., $T_{\rm LF}^{-1} \int_{0.5T_{\rm LF}}^{t^*} \Gamma'_{i,p} dt = \langle \Gamma'_{i,p} \rangle / 2$. Points A and B are shown in Fig. 2(b).

which is given by $\Gamma'_{i,p} = \Gamma_{i,p}/\langle \Gamma_{i,tot} \rangle$, where $\Gamma_{i,p}$ is the incident ion fluxes that collide with the powered electrode and $\langle \Gamma_{i,tot} \rangle$ is the time-averaged total ion fluxes that collide with both powered and ground electrodes over an RF cycle. Two cases are shown when $V_{LF} = 509$ V: (a) p = 0.4 Torr, $V_{HF} = 42$ V with $\gamma_i = 0.038$, and (b) p = 0.082 Torr, $V_{HF} = 500$ V with $\gamma_i = 0.02$, which correspond to Point A and B in Fig. 2(b).

A. Point A: p = 0.4 Torr, $V_{HF} = 42 V$, $V_{LF} = 509 V$ with $\gamma_i = 0.038$

The most important observation is that $\Gamma'_{i,p}$ has a phase lag with respect to the voltage waveform. When the powered electrode voltage is negative (i.e., $V_p < 0$ V), the ions are accelerated toward the powered electrodes; however, ions take time to reach the powered electrodes due to the ion inertia. The ion phase lag can be captured only in the self-consistent PIC-MCC simulation. During $V_p < 0$ V, the emitted electrons due to IIEE can be accelerated and then contribute to the ionization. On the other hand, during $V_p > 0$ V, emitted electrons from the powered electrodes can not go to the bulk region and go back to the powered electrode since the LF voltage is much larger than the electron temperature of IIEE, which means the IIEE does not affect the RF breakdown. In the E-MC simulation, electrons are emitted from the powered and grounded electrodes with equal probability; the half of IIEE affects the RF breakdown on average. On the other hand, less than half of the ions reach the powered electrodes when $V_p < 0$ V in the PIC-MCC simulation, leading to a smaller effective IIEE. This is the reason why a larger γ_i needs to be used in the PIC-MCC simulation to get similar breakdown voltages of E-MC simulation as shown in Fig. 2(b).

B. Point B: p = 0.082 **Torr,** $V_{HF} = 500 V$, $V_{LF} = 509 V$ with $\gamma_i = 0.02$

Interestingly, it can be seen from Fig. 3(a) that approximately half of the ions can reach the electrode during $V_p < 0$ V, which is equivalent to the assumption of IIEE in the E-MC simulation. Therefore, the HF breakdown voltages obtained from the PIC-MCC simulation are in better agreement with the E-MC simulation than Case (a) using $\gamma_i = 0.02$

VI. Conclusion

In this paper, the E-MC model and PIC-MCC model are developed for single- and dual-frequency RF breakdown. The breakdown characteristics obtained from E-MC simulation in good agreement with experimental data for both single- and dual-frequency RF breakdown. For single-frequency RF breakdown, the present E-MC simulations show that not only elastic reflection but also rediffusion and true secondary emission are important for the breakdown characteristics at lower voltages and lower pd. In addition, for the dual-frequency RF breakdown, the HF breakdown voltages are obtained when applying two constant LF voltages, $V_{\rm LF} = 283$ V and 509 V. The HF breakdown voltages obtained from the E-MC simulation are in good agreement with experimental data for both cases when accounting for the effective IIEE coefficient, $\gamma_i = 0.02$, and $\rho_e = 0.5$. IIEE is important in a wide range of pd values, and elastic reflection is important in the lower pd regime. On the other hand, the rediffusion and true secondary emission are not important for the dual-frequency RF breakdown.

The PIC-MCC simulation results are benchmarked with the E-MC simulation. The key difference between the PIC-MCC simulation and E-MC simulation is the timing of ion-induced electron emission. The electrons are emitted when ion collide with electrodes in the PIC-MCC simulation, while the timing of ion-induced electron emission is random in time in the E-MC simulation. The HF breakdown voltages obtained from the PIC-MCC simulation show good agreement with the E-MC simulation using the same ion-induced electron emission coefficient γ_i when $V_{\rm LF} = 283$ V. However, when $V_{\rm LF} = 509$ V, the PIC-MCC simulation results start to deviate from the E-MC simulation results using the same γ_i near the minimum voltages, and a higher γ_i is needed for the PIC-MCC simulation. The phase analysis of the incident ion flux reveals that the ion incident flux depends on the LF electric field, exhibiting a significant phase lag with respect to the voltage waveform. Consequently, the effective IIEE obtained from the PIC-MCC simulation is different from the E-MC simulation.

Acknowledgments

This material is based on work supported by the US Department of Energy, Office of Science, Office of Fusion Energy Sciences, under Award No. DE-SC0020623, the Office of Naval Research under Award No. N00014-21-1-2698, and Lam Research Corporation. The first author acknowledges the Japan Society for the Promotion of Science (JSPS) for the postdoctoral fellowship.

References

- [1] Yamashita, Y., Hara, K., and Sriraman, S., "Hysteresis between gas breakdown and plasma discharge," *Physics of Plasmas*, Vol. 31, No. 7, 2024.
- [2] Nishiyama, K., Hosoda, S., Tsukizaki, R., and Kuninaka, H., "In-flight operation of the Hayabusa2 ion engine system on its way to rendezvous with asteroid 162173 Ryugu," *Acta Astronautica*, Vol. 166, 2020, pp. 69–77.
- [3] Paschen, F., "Ueber die zum Funkenübergang in Luft, Wasserstoff und Kohlensäure bei verschiedenen Drucken erforderliche Potentialdifferenz," *Annalen der Physik*, Vol. 273, No. 5, 1889, pp. 69–96.
- [4] Boyle, W., and Kisliuk, P., "Departure from Paschen's law of breakdown in gases," *Physical Review*, Vol. 97, No. 2, 1955, p. 255.
- [5] Go, D. B., and Pohlman, D. A., "A mathematical model of the modified Paschen's curve for breakdown in microscale gaps," *Journal of Applied physics*, Vol. 107, No. 10, 2010.
- [6] Bilici, M. A., Haase, J. R., Boyle, C. R., Go, D. B., and Sankaran, R. M., "The smooth transition from field emission to a self-sustained plasma in microscale electrode gaps at atmospheric pressure," *Journal of Applied Physics*, Vol. 119, No. 22, 2016.
- [7] Lee, M. U., Lee, J., Lee, J. K., and Yun, G. S., "Extended scaling and Paschen law for micro-sized radiofrequency plasma breakdown," *Plasma Sources Science and Technology*, Vol. 26, No. 3, 2017, p. 034003.
- [8] Lisovskiy, V., Booth, J.-P., Landry, K., Douai, D., Cassagne, V., and Yegorenkov, V., "Low-pressure gas breakdown in dual-frequency RF electric fields in nitrogen," *Europhysics Letters*, Vol. 80, No. 2, 2007, p. 25001.
- [9] Puač, M., Marić, D., Radmilović-Radjenović, M., Šuvakov, M., and Petrović, Z. L., "Monte Carlo modeling of radio-frequency breakdown in argon," *Plasma Sources Science and Technology*, Vol. 27, No. 7, 2018, p. 075013.

- [10] Korolov, I., Derzsi, A., and Donkó, Z., "Experimental and kinetic simulation studies of radio-frequency and direct-current breakdown in synthetic air," *Journal of Physics D: Applied Physics*, Vol. 47, No. 47, 2014, p. 475202.
- [11] Korolov, I., and Donkó, Z., "Breakdown in hydrogen and deuterium gases in static and radio-frequency fields," *Physics of Plasmas*, Vol. 22, No. 9, 2015.
- [12] Walsh, J. L., Zhang, Y. T., Iza, F., and Kong, M. G., "Atmospheric-pressure gas breakdown from 2 to 100 MHz," Applied Physics Letters, Vol. 93, No. 22, 2008.
- [13] Yamashita, Y., Sharma, V., Sriraman, S., and Hara, K., "Electron Monte Carlo simulations of single-and dual-frequency RF breakdown," *Physics of Plasmas*, Vol. 32, No. 4, 2025.
- [14] Loveless, A. M., Breen, L. I., and Garner, A. L., "Analytic theory for field emission driven microscale gas breakdown for a pin-to-plate geometry," *Journal of Applied Physics*, Vol. 129, No. 10, 2021.
- [15] Chen, Z., Xu, J., Wang, H., Wu, H., Jiang, W., and Zhang, Y., "Influence of external circuitry on CF4 breakdown process in capacitively coupled plasma," *Journal of Vacuum Science & Technology B*, Vol. 41, No. 5, 2023.
- [16] Wu, H., Chen, Z., Yu, S., Wang, Q., Li, X., Jiang, W., and Zhang, Y., "The effects of match circuit on the breakdown process of capacitively coupled plasma driven by radio frequency," *Journal of Applied Physics*, Vol. 131, No. 15, 2022.
- [17] Bhattacharya, A., "Measurement of breakdown potentials and Townsend ionization coefficients for the Penning mixtures of neon and xenon," *Physical Review A*, Vol. 13, No. 3, 1976, p. 1219.
- [18] Abdel-kader, M. E., Gaber, W. H., Ebrahim, F. A., and Abd Al-Halim, M. A., "Characterization of the electrical breakdown for DC discharge in Ar-He gas mixture," *Vacuum*, Vol. 169, 2019, p. 108922.
- [19] Puač, M., Đorđević, A., and Petrović, Z. L., "Monte Carlo simulation of RF breakdown in oxygen—the role of attachment," *The European Physical Journal D*, Vol. 74, 2020, pp. 1–8.
- [20] Wu, H., Zhou, Y., Gao, J., Peng, Y., Wang, Z., and Jiang, W., "Electrical breakdown in dual-frequency capacitively coupled plasma: a collective simulation," *Plasma Sources Science and Technology*, Vol. 30, No. 6, 2021, p. 065029.
- [21] Semnani, A., Venkattraman, A., Alexeenko, A. A., and Peroulis, D., "Frequency response of atmospheric pressure gas breakdown in micro/nanogaps," *Applied Physics Letters*, Vol. 103, No. 6, 2013.
- [22] Radmilović-Radjenović, M., and Lee, J., "Modeling of breakdown behavior in radio-frequency argon discharges with improved secondary emission model," *Physics of plasmas*, Vol. 12, No. 6, 2005.
- [23] Furman, M., and Pivi, M., "Probabilistic model for the simulation of secondary electron emission," *Physical Review Special Topics—Accelerators and Beams*, Vol. 5, No. 12, 2002, p. 124404.
- [24] Phelps, A., and Pitchford, L., "Anisotropic scattering of electrons by N2 and its effect on electron transport," *Physical Review A*, Vol. 31, No. 5, 1985, p. 2932.
- [25] Vahedi, V., and Surendra, M., "A Monte Carlo collision model for the particle-in-cell method: applications to argon and oxygen discharges," *Computer Physics Communications*, Vol. 87, No. 1-2, 1995, pp. 179–198.
- [26] Mansour, A., Vialetto, L., Yamashita, Y., and Hara, K., "Electron inertial effects in the rarefied regime of a direct-current (DC) breakdown," *Plasma Sources Science and Technology*, Vol. 33, No. 11, 2024, p. 115018.